Adaptive Removal of the Transcranial Alternating Current Stimulation Artifact from the Electroencephalogram

Robert Guggenberger[1,*] and N.N.[1]

[1]Department for Translational Neurosurgery, University Hospital Tübingen
[*]Corresponding author: robert.guggenberger@posteo.eu

May 11, 2017

Abstract

Your abstract.

1 Introduction

The combination of transcranial alternating current stimulation (tACS) and electroencephalogram (EEG) has been explored in several recent studies. While the analysis of EEG before or after stimulation posits limited technical challenges, the EEG recording during stimulation is heavily affected by the stimulation artifact.

1.1 Matched Phase and Frequency

Computational simulations suggest that the power of endogenous oscillations would increase most if the frequency of tACS matches the targets eigenfrequency (Kutchko and Fröhlich, 2013; Zaehle et al., 2010). This has been supported by evidence from animal studies (Schmidt et al., 2014), and human studies combining tACS with transcranial magnetic stimulation (TMS) (Guerra et al., 2016), or contrasting pre and post resting state power analysis (Zaehle et al., 2010). It has also been suggested that the phase of neuronal populations would be locked to the phase of the tACS signal (Reato et al., 2013). This has been supported by evidence from studies combining tACS with motor output (Brittain et al., 2013), TMS (Raco et al., 2016; Nakazono et al., 2016) or sensory perception (Gundlach et al., 2016).

This suggests that the effect of tACS can result in neurophysiological effects which are phase-and frequency-matched to the stimulation artifact. Such frequency and phase matching between tACS and EEG recordings can render the removal of the artifact difficult or impossible, as the signal might no longer be separatable from the artifact.

1.2 Non-Stationary Amplitude Modulation

An approach to tackle this issue is to assess the time-course of the EEG signal. Consider the assumption that the artifact is stationary and superpositioned on the physiological signal. Then, modulations in the amplitude of the recorded EEG-signal must be caused by changes in the underlying physiology. This would be the case, even if frequency and phase are matched to the stimulation signal. Approaches assuming such stationarity of the stimulation artifact have been used e.g. by Pogosyan et al. (2009).

Yet, detailed analysis of the stimulation artifact provides evidence that the artifact amplitude is actually not stationary. Instead, the amplitude is modulated by heart-beat and respiration (Noury et al., 2016). Recently, non-linearities in how stimulators control the applied current has been suggest as further source of modulation (Neuling et al., 2017). It has been argued that unregularized spatial filters might be able to remove this amplitude modulation (Neuling et al., 2017). But if only few channels are recorded, the method can fail, as the estimation of the spatial covariance is insufficient, or impossible in the single-channel-case.

Consider furthermore that event-related responses like modulation of skin impedance can also affect the scalp conductance at stimulation electrodes. This would introduce event-related amplitude modulation of the stimulation artifact. In that regard, disentangling true signal from the stimulation artifact stays technically challenging.

1.3 Artifact Distortion

Ideally, the stimulation artifict of tACS resembles a sinusoid. Yet, practical experience suggests that the signal is usually distorted to various degrees. Figure 1 shows examples of distortion and saturation in two recordings of tACS-EEG. The gray traces indicate nine invididual periods, while the red trace indicates their average. In figure 1a, note the periodic, yet non-sinusoidal waveform. In figure 1b, note the saturation.

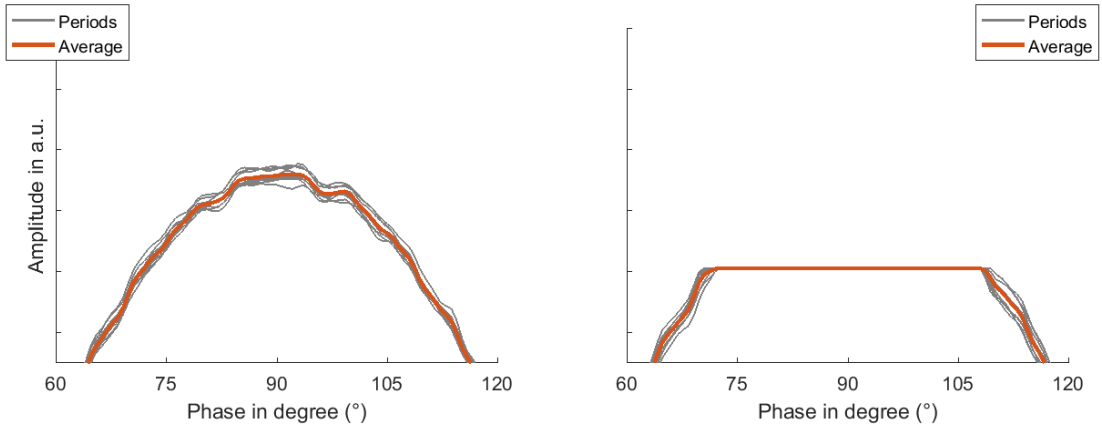

(a) Distortion

(b) Saturation

Figure 1: Examples for loss of sinusoidal fidelity

The temporally and spatially uneven impedance distribution has been suggested as cause of distortion, rendering the resulting waveform periodic, but non-sinusoidal. A major problem is amplifier saturation, i.e. the stimulation artifact exhibiting an amplitude to large for the dynamic range of the amplifier, causing the signal to be cut off and information to be lost. Additionally, non-linearites in the amplifier slew rate can distort the shape even when the signal is close to the saturation threshold.

1.4 Computational Demands

Methods based on adaptive template construction and temporal principal component analysis (tPCA) (Niazy et al., 2005) have been explored for removal of non-stationary and misshaped tACS artifacts (Helfrich et al., 2014). Consider that the process of template construction, the estimation of accurate weights for removal by template subtraction and the suqsequent removal of residual artifacts using tPCA is computationally cumbersome. Additionally, it often requires off-line analysis supported by visual inspection. Such a multi-staged template-approach is therefore of limited utility for on-line artifact removal. Furthermore, critical evaluation has suggested that the residual artifact spans several principal components, and a sufficient artifact removal is therefore not possible with tPCA (Noury et al., 2016).

1.5 Motivation

We were interested in development of a computationally fast approach, feasible for online artifact removal. At the same time, the approach was required to account for the dynamical modulation of the artifact amplitude, and the possibility of non-sinusoidal distortion and saturation. Ideally, the approach would allow to derive physiological signals at the frequency of stimulation, even if physiological oscillations were phase-locked to the stimulation signal. Furthermore, the approach should be usable offline, as to allow recovery of information from already collected datasets.

2 Approach

The main idea is that at any given time point t, the recorded signal $r(t)$ is a linear superposition of a neurophysiological signal $n(t)$, the stimulation artifact $a(t)$ and a white noise term $e(t)$. The task is to recover $n(t)$ by estimating $\hat{a}(t)$ and $e(t)$ and subtracting from $r(t)$.

$$r(t) = n(t) + a(t) + \epsilon(t) \tag{1}$$
$$n(t) = r(t) - \hat{a} - \epsilon(t) \tag{2}$$

2.1 Periodic Estimation

Assume that the tACS artifact were non-sinusoidal, but stationary and periodic. At the same time, assume that neurophysiological signals n and noise ϵ were absent. Then, we could estimate the amplitude of a at any time-point t by using the signal r recorded from any time-point, as long as this time-point is an integer multiple of the artifacts period length p earlier (3). Subtraction of a delayed version of the signal is also known as comb filter. Please note that for discretely sampled signals, this approach natively supports only frequencies which are integer divisibles of the sampling frequency. If this is not the case, upsampling the recorded signals to an appropriate sampling rate, comb filtering, and downfiltering is a viable approach.

$$\hat{a}(t) = r(t - np) \tag{3}$$
$$n \in \mathbb{Z} \tag{4}$$

2.1.1 Uniform Comb Filter

Consider that the noise term ϵ is still superpositioned on r. If the noise term were white, and because the expectation of white noise $\langle\epsilon\rangle$ converges asymptotically to zero with increased sample size, an approach to estimate a bias-free artifact amplitude would be to average across as many earlier periods as possible (5). Subsequently, this estimate can be used to remove the artifact from r. In real applications, stimulation duration is limited and computational constraints exist. This is reflected by the fact that we have to use a finite number for N.

$$\hat{a}(t) = \sum_{n=1}^{N} \frac{r(t - np)}{N} \tag{5}$$

2.1.2 Superposition of Moving Averages

Please note that averaging across neighbouring periods M (6) has been suggested before and termed superposition of moving averages (SMA) by Kohli and Casson (2015).

$$\hat{a}(t) = \sum_{n-M/2}^{n+M/2} \frac{r(t - np)}{M + 1} \tag{6}$$

Consider that the approach using only past values (5) returns a causal filter. Applied online, a causal filter would be able to remove the artifact without the delay of $(Mp)/2$ necessary for SMA. Furthermore, SMA is well-defined only for even M. This motivates the exploration of causal filters for artifact removal.

2.2 Temporal Weighting

Consider that the amplitude of the artifact has been described to be non-stationary and dynamically modulated (Noury et al., 2016; Neuling et al., 2017). Although it has been suggested that there are event-dependent components of the amplitude modulation (e.g. by heartbeat or respiration Noury et al. (2016) or stimulator impedance check Neuling et al. (2017)), the parameters of the dynamical system governing event-independent amplitude modulation are usually not known a priori.This can render online artifact removal problematic.

One approach to tackle this problem is to use instead of a constant weight $1/N$ (5), a time-dependent weighting function w_n (7).

$$\hat{a}(t) = \sum_{n=1}^{N} w_n r(t - np) \tag{7}$$

By controlling the parameters of the weight functions, can we attempt to match the process governing the amplitude modulation This might allow us to achieve a better artifact estimation and subsequent removal. Please note that if the reliability of past periods can be estimated, we might select weights empirically. [1] Yet, these approaches require extended calculation periods and/or offline analysis. In the following sections, we will discuss and justify three predeterminable weighting functions feasible for fast online-filtering.

2.2.1 Justification by Sampling

Consider for example the simple one-step comb filter, where we remove the artifact by subtracting a value sampled from any earlier period. Assume now that this value were not drawn from the last period, but instead drawn at random from the last N periods with uniform distribution. If the system governing amplitude modulation were fully stationary for the last N periods, performance would in law be virtually identical to the comb filter based on averaging (5). If it were instead non-stationary, we would expect that the precision of the estimate degrades with longer delay. For example, in the case of the uniform filter, we have a shape parameter N, defining how far back we trust a measurement to have the same precision as earlier samples. This rationale justifies non-uniform weights, and to use weights that are linked to the precision of the sample.

2.2.2 Justification by AR (1) process

Consider that the system governing the amplitude of the stimulation artifact could be decomposed into the constant amplitude c controlled by the stimulator and a dynamical, event-unrelated process governing the amplitude modulation. If we model this process as an AR (1) process, this would return for N approaching infinity:

$$X_t = c + \sum_{n=0}^{\infty} \phi_n \epsilon_{t-k} \tag{8}$$

If the kernel Φ behind the modulation of the artifacts amplitude were known, or could be estimated sufficiently, we could construct an optimal weighting function as a deconvolution filter. This line of reasoning is based on the similarity between the generic weighted comb filter (7) and the generic discrete-time AR (1) process (8). Note that, for practical applications, we would need finite N. This would limit the application to kernels decaying sufficiently fast.

[1] An offline method based on estimation of reliability using the autocorrelation has been implemented in the toolbox.

2.3 Temporal Weighting Examples

2.3.1 Linear Weighting

One straight-forward approach is using a linear decreasing weighting function. The assumption of local linearity is widely used in the analyis of non-linear dynamical systems, which could render the kernel sufficiently flexible. Additionally, the function is simple and the necessary normalization can easily be calculated by using the triangular number for a given N as normalizing constant k (10). Hence, equation (9) returns weights for earlier periods based on a linear temporal weight decay.

$$w_n = \frac{N - n + 1}{k} \tag{9}$$

with the following normalization

$$k = \sum_{n=1}^{n} n = \frac{N(N+1)}{2} \tag{10}$$

2.3.2 Exponential Weighting

Motivated by the fact that the autocorrelation function of an AR (1) process can be expressed as a decaying exponential, an alternative approach would be an exponential weighting function. The time constant τ of an exponential controls its temporal decay. To maintain the shape across different N, we consider it reasonable to normalize n by N. Hence, equation (11) returns weights for earlier periods based on their exponential temporal weight decay.

$$w_n = \frac{1}{k} e^{\tau - \tau(n/N)} \tag{11}$$

with the following normalization

$$k = \sum_{n=1}^{N} e^{\tau - \tau(n/N)} \tag{12}$$

2.3.3 Gaussian Weighting

Consider that the amplitude modulation might be governed by more than one AR (1) process, or the process might be non-stationary itself. Motivated by the fact that such sums often converge to a normal distribution, an alternative approach would be a Gaussian weighting function. Using a suitable parameterization, and centering on zero, the inverse of the standard deviation $\frac{1}{\sigma^2}$ defines the time constant τ of a Gaussian distribution, which controls its temporal decay. To maintain the shape across different N, we consider it again reasonable to normalize n by N. Hence, equation (13) returns weights for earlier periods based on their Gaussian temporal weight decay.

$$w_n = \frac{1}{k} f(n/N) \tag{13}$$

with the following generating function and normalization

$$f(x) = \sqrt{\frac{\tau}{2\pi}} e^{-(\tau x^2)/2} \tag{14}$$

$$k = \sum_{n=1}^{N} f(n/N) \tag{15}$$

2.4 Alternative Filter Approaches

2.4.1 Adaptive Discrete Fourier Transformation

2.4.2 Adaptive Removal of Principal Components

3 Evaluation

We implemented functions for kernel creation and artifact removal in Matlab 2016b. Code[2] can be accessed online. We evaluated the behavior of the various kernels regarding their frequency response characteristics (see 3.1) as well as their behavior on simulated (see 3.2) and real data (see 3.3).

3.1 Evaluation of Frequency Response

Examine the following exemplary kernels constructed for a sampling rate of 1KHz, a stimulation frequency of 10 Hz and a memory of 10 (see figure 2).

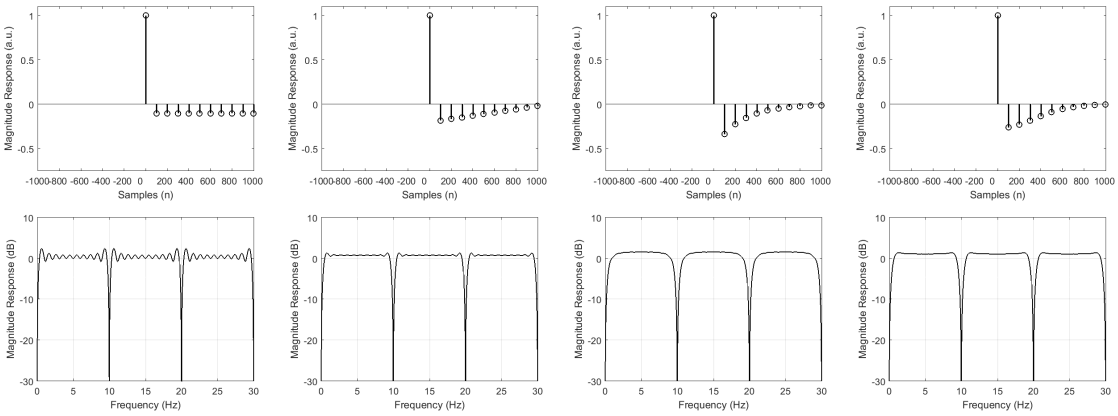

(a) Uniform (b) Linear (c) Exponential $\tau = 4$ (d) Gaussian $\tau = 3$

Figure 2: Exemplary Causal Kernels

As you can see from figure 2, the (numerically calculated) magnitude responses of the four approaches are highly similar. Their key characteristic is the strong supression of the target frequency and its integer multiples. Yet, note the difference in passbands. We find strong ringing in the passband for the uniform (2a) and linear kernel (2b), especially compared to the smooth transitions of the exponential (2c) or Gaussian kernel (2d).

We constructed a set of exponential kernels constructed with different τ and N to explore their behavior (see figure 3). We find it of note that that in the limiting case of $\tau = 0$, the exponential kernel virtually converges with the uniform kernel (see figure 3a). Using a τ equal to the artifacts period length, the exponential kernel almost fully converges with the simple comb filter (see figure 3c). Note also that very high τ would return an impulse response, and therefore just pass all signals. This is also true for the limiting case of $N = 1$, were we would again acquire a simple comb filter. By increasing N we achieve a flattening of the pass-band gain (see figure 3d).

3.2 Evaluation on Simulated Signals

To evaluate the filters, we tested them on simulated signals. The simulated signal was created as superposition of a 10 Hz tACS-artifact, and an event-related potential (ERP).

[2] `https://github.com/agricolab/ARtACS`

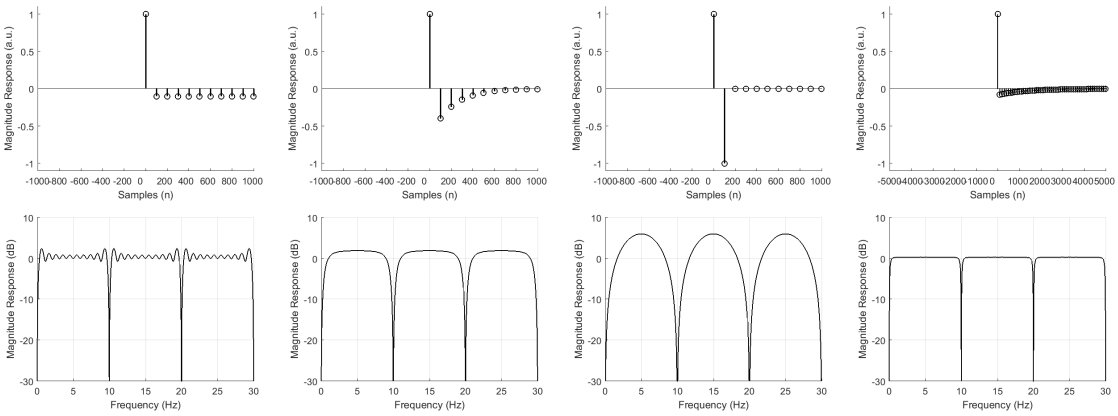

(a) $\tau = 0, N = 10$ (b) $\tau = 5, N = 10$ (c) $\tau = 100, N = 10$ (d) $\tau = 4, N = 50$

Figure 3: Exemplary τ and N Tuning

(a) Experimental Setup

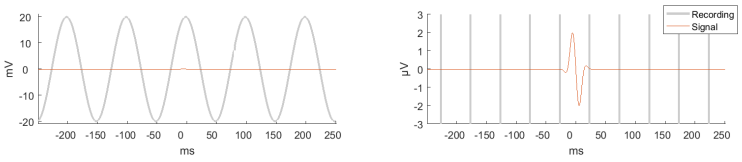

(b) Signal Comparison

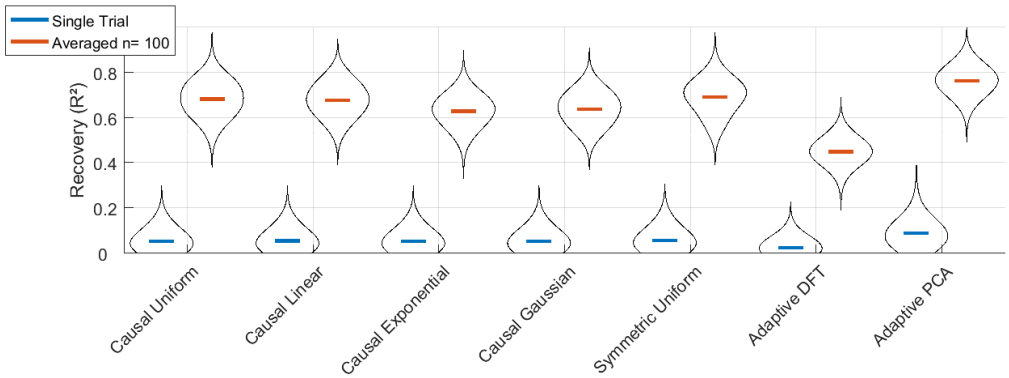

(c) Kernel Density Estimation of R^2 for different filter approaches

Figure 4: Overview for Artifact Removal from Simulated Signal

The ERP was simulated as numerical gradient of a flat top window. The amplitude of the artifact was simulated as a distorted, non-stationary sinusoidal. The initial stimulation signal was modelled as sinusoidal signal. We distorted it by adding periodic white noise. Additionally, the stimulation amplitude was driven by an Ornstein–Uhlenbeck, i.e. AR (1), process with a stiffness 0.5, and a Hanning window time-locked to the event- related potential.

In that way, we were able to simulate event-independent modulations of the artifacts amplitude, and modulations locked to an event. Such effects were described by (Noury et al., 2016), as having a strong potential to mask the true event-related neurophysiological activity.

Subsequently, we explored different filter approaches, i.e. the two times four causal and symmetric weighted comb filters, all with a period number of 10. Additionally we evaluated adaptive discrete fourier filtering with the same period length of 10, and a linear regression of the artifact based on a copy of the efferent stimulation signal, as one could acquire from the tACS-stimulator, e.g. the NeuroConn DC Plus.[3]

We simulated 100 trials. Based on the correlation of the filtered, artifacted recording with the simulated underlying signal, we calculated the R^2 value. Blue bars indicate the average R^2 for single-trial reconstructions, and red bars the average R^2 for boot-strapped grand-average ERPs (see figure 4c).

Visual inspection of the R^2 estimates shows that all filtering approaches are able to recover at least some information about the ERP. Differences between the comb filters is small.

3.3 Evaluation on real data

To evaluate the filters, we tested them on real physiological signals. Consider that tACS can have physiological effects on cortical ERP. To properly evaluate the recovery using the filtering approaches, we need a physiological signal which is unlikely to be affected by tACS.

We therefore measured electrocardiogram (ECG) close to the flexor digitorum of the left upper limb, while we stimulated distal and proximal with tACS to the muscle belly with 11 Hz at 1 mA. We also recorded ECG at the chest, and detected the R-peak for epoching the data. Please note that no tACS-artifact was visible in the chest ECG. Physiological signals were acquired using BrainProducts amplifiers at a sampling rate of 1 kHz and low-pass filtered below 35 Hz. Stimulation as delivered using a NeuroConn DC Stimulator Plus with carbon rubber electrodes and Ten20 electrode gel.

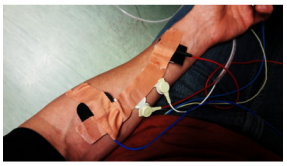

(a) Experimental Setup

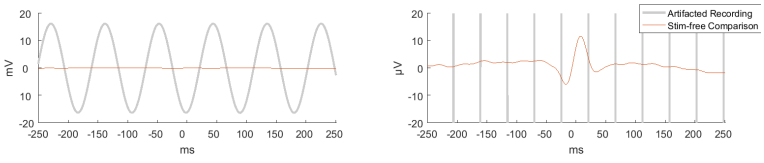

(b) Signal Comparison

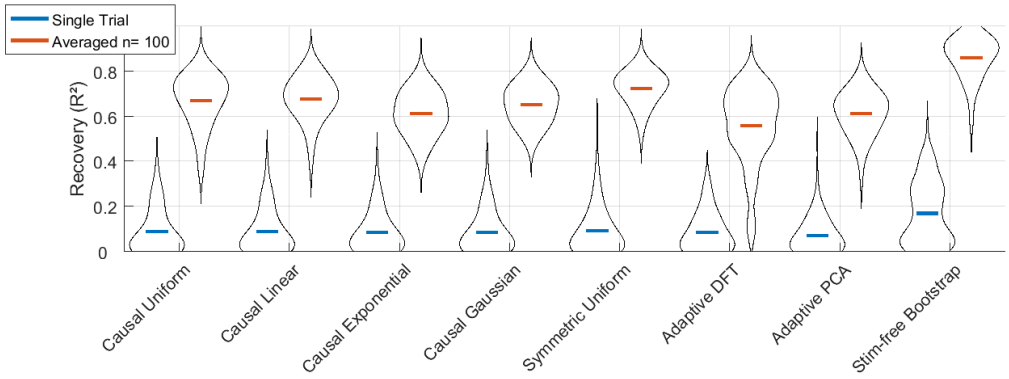

(c) Kernel Density Estimation of R^2 for different filter approaches

Figure 5: Overview for Artifact Removal from Upper Limb Electrocardiogram

[3]Code can be found at `https://github.com/agricolab/ARtACS`

We recorded a total of 134 R-peaks without stimulation and 136 with stimulation. Based on the correlation of the filtered, artifacted recordings with the grand-average of the stimulation-free signal, we calculated the R^2 value. Blue bars indicate the average R^2 for single-trial reconstructions, and red bars the average R^2 for boot-strapped grand-average ERPs based on 100 epochs (see figure 5c).

4 Conclusion

References

Brittain, J.-S., Probert-Smith, P., Aziz, T. Z., and Brown, P. (2013). Tremor suppression by rhythmic transcranial current stimulation. Current Biology, 23(5):436–440, DOI: 10.1016/j.cub.2013.01.068.

Guerra, A., Pogosyan, A., Nowak, M., Tan, H., Ferreri, F., Lazzaro, V. D., and Brown, P. (2016). Phase dependency of the human primary motor cortex and cholinergic inhibition cancelation during beta tACS. Cerebral Cortex, 26(10):3977–3990, DOI: 10.1093/cercor/bhw245.

Gundlach, C., Müller, M. M., Nierhaus, T., Villringer, A., and Sehm, B. (2016). Phasic modulation of human somatosensory perception by transcranially applied oscillating currents. Brain Stimulation, 9(5):712–719, DOI: 10.1016/j.brs.2016.04.014.

Helfrich, R. F., Schneider, T. R., Rach, S., Trautmann-Lengsfeld, S. A., Engel, A. K., and Herrmann, C. S. (2014). Entrainment of brain oscillations by transcranial alternating current stimulation. Current Biology, 24(3):333–339, DOI: 10.1016/j.cub.2013.12.041.

Kohli, S. and Casson, A. J. (2015). Removal of transcranial a.c. current stimulation artifact from simultaneous EEG recordings by superposition of moving averages. In 2015 37th Annual International Conference of the IEEE Engineering in Medicine and Biology Society (EMBC). IEEE, DOI: 10.1109/embc.2015.7319131.

Kutchko, K. M. and Fröhlich, F. (2013). Emergence of metastable state dynamics in interconnected cortical networks with propagation delays. PLoS Computational Biology, 9(10):e1003304, DOI: 10.1371/journal.pcbi.1003304.

Nakazono, H., Ogata, K., Kuroda, T., and Tobimatsu, S. (2016). Phase and frequency-dependent effects of transcranial alternating current stimulation on motor cortical excitability. PLOS ONE, 11(9):e0162521, DOI: 10.1371/journal.pone.0162521.

Neuling, T., Ruhnau, P., Weisz, N., Herrmann, C. S., and Demarchi, G. (2017). Faith and oscillations recovered: On analyzing EEG/MEG signals during tACS. NeuroImage, 147:960–963, DOI: 10.1016/j.neuroimage.2016.11.022.

Niazy, R., Beckmann, C., Iannetti, G., Brady, J., and Smith, S. (2005). Removal of FMRI environment artifacts from EEG data using optimal basis sets. NeuroImage, 28(3):720–737, DOI: 10.1016/j.neuroimage.2005.06.067.

Noury, N., Hipp, J. F., and Siegel, M. (2016). Physiological processes non-linearly affect electrophysiological recordings during transcranial electric stimulation. NeuroImage, 140:99–109, DOI: 10.1016/j.neuroimage.2016.03.065.

Pogosyan, A., Gaynor, L. D., Eusebio, A., and Brown, P. (2009). Boosting cortical activity at beta-band frequencies slows movement in humans. Current Biology, 19(19):1637–1641, DOI: 10.1016/j.cub.2009.07.074.

Raco, V., Bauer, R., Tharsan, S., and Gharabaghi, A. (2016). Combining TMS and tACS for closed-loop phase-dependent modulation of corticospinal excitability: A feasibility study. Frontiers in Cellular Neuroscience, 10, DOI: 10.3389/fncel.2016.00143.

Reato, D., Rahman, A., Bikson, M., and Parra, L. C. (2013). Effects of weak transcranial alternating current stimulation on brain activity—a review of known mechanisms from animal studies. Frontiers in Human Neuroscience, 7, DOI: 10.3389/fnhum.2013.00687.

Schmidt, S. L., Iyengar, A. K., Foulser, A. A., Boyle, M. R., and Fröhlich, F. (2014). Endogenous cortical oscillations constrain neuromodulation by weak electric fields. Brain Stimulation, 7(6):878–889, DOI: 10.1016/j.brs.2014.07.033.

Zaehle, T., Rach, S., and Herrmann, C. S. (2010). Transcranial alternating current stimulation enhances individual alpha activity in human EEG. PLoS ONE, 5(11):e13766, DOI: 10.1371/journal.pone.0013766.